Blends of Polypropylene Resins with a Liquid Crystalline Polymer. I. Isothermal Crystallization

A. L. Marinelli, R. E. S. Bretas

Department of Materials Engineering, Universidade Federal de São Carlos, 13565-905 São Carlos, SP, Brazil

Received 1 June 2001; accepted 8 January 2002

ABSTRACT: The isothermal crystallization kinetics of blends of different polypropylene (PP) resins and a liquid crystalline polymer (LCP) after two different melting conditions (200 and 290°C) were studied by DSC and polarized light optical microscopy. The resins were a homopolymer (hPP), a random copolymer with ethylene (cPP), and a maleic anhydride grafted PP (gPP). The LCP was Vectra A950, a random copolymer made of 75 mol % of 4-hydroxybenzoic acid and 25 mol % of 2-hydroxy,6-naphthoic acid. It was observed that the overall crystallization rates of all the blends after melting at 200°C were higher than those after melting at 290°C. The LCP acted as a nucleating agent for all the PP resins; however, its nucleating effect was stronger for the hPP than for the cPP and gPP resins. After both melting conditions, an increase was observed in the overall crystallization rate of the hPP and gPP resins with the increase in the amount of LCP, but not in the cPP crystallization rate. The fold surface free energy σ_e of hPP and cPP in the blends decreased, but increased in the gPP blends. Finally, all the PP resins formed transcrystallites on the LCP domain surfaces. © 2002 Wiley Periodicals, Inc. J Appl Polym Sci 87: 916–930, 2003

Key words: crystallization; nucleation; mechanical properties; liquid-crystalline polymers (LCPs); polypropylene (PP)

INTRODUCTION

Liquid crystalline polymers (LCPs) have outstanding mechanical properties, with elastic modulus ranging between 15 and 100 GPa,[1] depending on the processing conditions. However, their major drawback is their high cost. On the other hand, polypropylene is a commodity thermoplastic, of low cost and low elastic modulus. Thus, the blending of these two polymers could produce a composite of lower cost than that of the LCP and higher elastic modulus than that of the PP, for example. For that reason, blends of PP with LCPs have been widely studied,[2–4] mainly to find correlations between processing conditions and mechanical properties.

It has been found,[2] for example, in blends of PP and LCP, that the addition of maleic anhydride (MA)–grafted polypropylene to the PP matrix increases the mechanical properties of these blends and increases the dispersion of the LCP phase, thus reducing the interfacial tension. It has also been concluded from that study[2] that the MA does not react with the LCP and that interactions like hydrogen bonding between the MA and the LCP are responsible for the compatibilization. In another study,[3] in which microcomposites of PP and LCP were produced at temperatures below the melting temperature of the LCP, to preserve the properties and structure of the pregenerated LCP fibers, it was found that the mechanical properties of microcomposites, processed at temperatures where the LCP behaved like solid fibers, were more balanced than were the *in situ* composites formed by melting both the LCP and the PP. However, in that study[3] it was also found that the modulus of the microcomposites was lower than the modulus predicted by the composite theory, probably because the LCP fibrils have a low aspect ratio and a poor distribution within the PP phase. Another study[4] found that optimum mechanical properties in these blends were achieved when the LCP/PP viscosity ratio ranged between 2 and 4, at $T = 285$°C and shear rates between 800 and 1000 s^{-1}.

Therefore, besides the usual processing conditions, two parameters seem to exert a significant influence on the mechanical properties of the PP/LCP blends: (1) the processing temperature of the blends (above or below the LCP melting point) and (2) the compatibilization of the two components.[5] The mechanical properties, on the other hand, are also dependent on the degree of PP and LCP crystallinity achieved during the cooling and on the interfacial adhesion promoted by the compatibilizer.

For that reason, the crystallization kinetics of these blends have also been studied[6–9] by other authors. One study[6] found that the LCP acted as a nucleating agent for the PP, increasing the crystallization temper-

Correspondence to: R. E. S. Bretas (bretas@power.ufscar.br).
Contract grant sponsor: PRONEX.
Contract grant sponsor: FAPESP.

ature and the degree of crystallinity of the PP; PP transcrystallinity around the LCP particles and the formation of more homogeneous PP spherulites were observed. This more homogeneous PP morphology was attributed to suppression by the LCP, of the formation of the β-phase of the PP. The isothermal and nonisothermal crystallization of these blends, compatibilized with MA, have also been studied[7]; the authors found that the PP spherulite size decreased with the LCP addition, and that the compatibilization with MA promoted a finer dispersion of the LCP phase in the PP matrix. Again, transcrystallinity and LCP nucleation of the PP were observed, and the rate of crystallization was enhanced in the PP/LCP compatibilized blends. Miteva and Minkova,[8] using a PP-*g*-LCP copolymer as a compatibilizer, studied its influence on the crystallization behavior, crystal structure, and morphology of PP/LCP blends. This compatibilizer was made of long PP and LCP segments, preserving the crystalline nature of the pure components. They concluded that the PP segments of the compatibilizer can cocrystallize with the PP of the blend and the LCP segments of the compatibilizer can also cocrystallize with the LCP of the blend, or even enter the amorphous phase of the blends; therefore each part of the compatibilizer seems to be miscible with the corresponding component in the blend. The migration of the compatibilizer to the interphase thus led to an increase of the PP crystallization rate (by increasing the nucleation rate), to a decrease in the PP spherulites' dimensions and to an increase in the PP percentage of crystallinity. The isothermal crystallization of these blends was also studied,[9] in a temperature range in which the LCP remained in the solid state. Again, it was observed that the addition of the compatibilizer increased dramatically the overall crystallization rate of the PP in the blend and decreased the LCP size in the blend.

In the present investigation, the isothermal crystallization of PP/LCP blends was studied after two melting conditions: (1) at a temperature in which only the PP was melted (200°C) and (2) at a temperature at which both PP and LCP were melted (290°C).

EXPERIMENTAL

Materials

Three different PP resins were used: a homopolymer (hPP), a random copolymer with 3% ethylene (cPP), and a grafted copolymer with 0.15% of maleic anhydride (gPP). The first two were kindly donated by OPP Petroquímica of Brazil and the last one was bought from Uniroyal. The molecular weight (MW) and the melt flow index (MFI) of these resins are given in Table I.

The LCP used was Vectra A950, a random copolymer made of 75 mol % of 4-hydroxybenzoic acid (HBA) and 25 mol % of 2-hydroxy, 6-naphthoic acid (HNA)[10,11] from Ticona, without antioxidants. To avoid thermal degradation of the gPP resin, an antioxidant compound made of Irgafos 168 and Irganox 1010, in a ratio of 2 : 1, was used.

TABLE I
PP Resins Used in This Work

Resin	MW (g/mol)	MFI (g/10 min)
hPP	470,000	10
cPP	240,000	10
gPP	—	5

The chemical structure of the PP resins was also confirmed by use of a Perkin–Elmer FTIR Spectrum model 100 (Perkin–Elmer, Palo Alto, CA); for these studies films of 30 μm, made by hot pressing at 150°C, were used.

Preparation of the blends

The PP and LCP resins were dried at 100°C for 24 h before mixing. Each composition was first tumbled together in a container on a weight ratio basis (30, 50, and 70% LCP) and then injection molded. The injection molding was made in a Pic-Boy machine (hPP/LCP and cPP/LCP blends) and in Arburg 270 equipment (gPP/LCP blends). The temperature of zone 1 of the injection molding machines was 290°C and of zone 2 was 295°C; the mold was kept at room temperature.

Degradation studies

Because of the high melting temperatures and high shear rates used in the processing of these blends, some degradation studies were necessary: a stress-controlled rheometer (Model SR-200; Rheometrics) was used for these studies. Measurements of the complex viscosity $[\eta^*(\omega)]$ as a function of time, at 200 and 290°C, were done on the virgin PP resins, in a parallel-plates geometry, at a frequency of 10 Hz, with a shear stress of 500 Pa under N_2 atmosphere.

Isothermal crystallization

Avrami analysis from DSC

The isothermal crystallization of homopolymers can be described by the Avrami equation,

$$\ln\{1 - (X_c(t)/X_\infty)\} = -kt^n \quad (1)$$

where X_c is the degree of crystallinity as a function of time, X_∞ is the ultimate crystallinity, and n and k are Avrami parameters.

As known,[12] n can be related to the nucleation type, morphology, and dimensionality of the crystals devel-

oped during the crystallization, and k is related to the overall crystallization rate G because $k \propto G^n$.

For the isothermal studies, a Perkin–Elmer DSC-7 differential scanning calorimeter was used. In these experiments, an indium standard was used for temperature calibration; nitrogen atmosphere was also used in all the scans.

These DSC studies were divided in four parts:

1. Heating the pure components at 20°C/min to obtain their respective melting temperatures, $T_{m,\mathrm{PP}}$ and $T_{m,\mathrm{LCP}}$; these temperatures were 164.4, 152.4, and 166.6°C for the hPP, cPP, and gPP resins, respectively, and 290°C for the LCP. On the basis of these values, melting temperatures (T_m) of 200 and 290°C were chosen to perform all subsequent heating and cooling experiments.
2. Heating the pure components at 20°C/min up to T_m values of 200 and 290°C; holding at these temperatures for 5 and 2 min, respectively; and cooling down at −10°C/min to room temperature. The PP resins' cold crystallization temperatures were observed to be between 108 and 122°C; however, after melting at 290°C, the LCP cold crystallization temperature was not detected. Langelaan and de Boer[13] found that, at 290°C, this particular LCP melts quickly and recrystallizes slowly; therefore, 290°C is a temperature at which melting and recrystallization of the LCP can occur. Thus, another T_m = 330°C was used, only for the LCP; this time, a cold crystallization temperature of 238°C was observed. However, T_m = 330°C was not used in the experiments because, at this temperature, the PP resins would quickly degrade.
3. Heating of the blends at 20°C/min up to 200°C, holding for 5 min at this T_m, cooling down at −105°C/min to the isothermal crystallization temperature (T_c), and holding at this last temperature until the crystallization process was finished. The chosen T_c values were 116, 118, 120, and 122°C. At T_m = 200°C, only PP was melted. The percentage of PP crystallinity $X_{c,\mathrm{PP}}$ was calculated using the following equation:

$$X_{c,\mathrm{PP}} = \Delta H_{c,\mathrm{PP}} / w\, \Delta H^{\circ}_{m,\mathrm{PP}} \quad (2)$$

   where $\Delta H_{c,\mathrm{PP}}$ is the heat of PP crystallization, $\Delta H^{\circ}_{m,\mathrm{PP}}$ is the heat of 100% crystalline PP = 209 J/g,[14] and w is the weight fraction of the PP in the blend.
4. Heating of the blends at 20°C/min up to 290°C, holding for 2 min at this temperature, cooling down at −105°C/min to the above-mentioned T_c value, and holding at this last temperature until the crystallization process was finished. At T_m = 290°C, the LCP melted and then recrystallized. Again, $X_{c,\mathrm{PP}}$ was calculated using eq. (2).

The equilibrium melting temperature of the PP (T°_m) was measured by using the standard Hoffmann–Weeks procedure.[15] T°_m is defined[16] as the temperature at which an assembly of crystals, large enough that surface effects are negligible, is in equilibrium with the normal polymer liquid; these crystals also must have an equilibrium degree of perfection consistent with the minimum free energy at T°_m. Therefore, its depression can be a consequence of blend miscibility. To obtain an extended temperature range, isothermal crystallization temperatures higher than 120°C were used, given that near this last temperature, PP recrystallization can occur.[17,18]

Spherulite isothermal linear growth rate (G_g) by polarized light optical microscopy (PLOM)

To observe the blends' final morphology, and to determine the isothermal linear growth rate of the PP spherulites in the blends (G_g), experiments were carried out by PLOM. The PLOM was from Leica (model DMRXP; Leica Imaging Systems, Cambridge, UK), with a hot stage from Linkam (model THMS 600). To the microscope, a video camera Kappa was attached and the spherulitic growth of the samples recorded by video equipment. The melting and crystallization temperatures used were the same as those used in the DSC experiments; the cooling rate, however, was −130°C/min. The calibration of the sample temperature was made by using an Fe–Co thermocouple with a junction of 60 μm, put directly into the polymeric sample. The growth rate of each sample was calculated by measuring the slopes of the spherulites' radius versus time curves.

Glass-transition temperature (T_g) by dynamic mechanical thermal analysis (DMTA)

The T_g values of the samples were measured by use of a dynamic mechanical analyzer (DMTA, model MkII; Polymer Laboratory, UK), in the bending mode, single cantilever, at 1 Hz and 64 μm of strain. The samples were heated at 4°C/min. The T_g value was assumed to be the temperature at which the loss modulus E'' had a maximum; the other found transitions, T_β and $T_{\alpha'}$, corresponded to observed transitions below T_g and above T_g, respectively. Therefore, T_β represents low range molecular relaxations, like crankshaft movements, and $T_{\alpha'}$ represents the relaxation of the amorphous parts of intracrystallites. In the case of the Vectra A950, T_β was attributed[19] to the relaxation of the naphthyl groups of the HNA comonomer.

Fold interfacial free energy (σ_e)

The value of G_g can also be used to calculate the fold interfacial free energy σ_e. G_g is related to the degree of

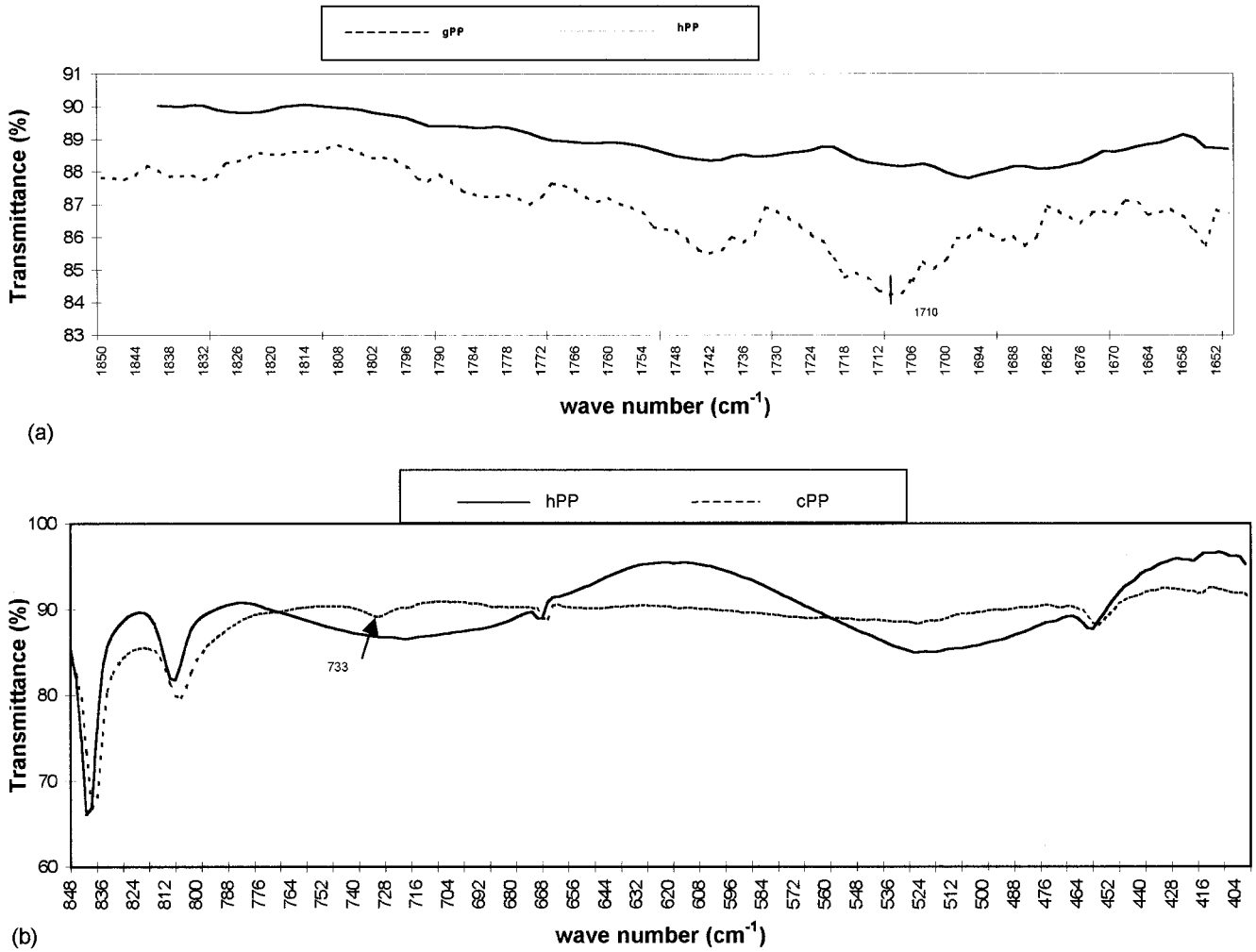

Figure 1 FTIR spectra of the pure polypropylenes: (a) gPP and hPP; (b) cPP and hPP.

undercooling (ΔT) by the traditional equation of Hoffman and coworkers[20]:

$$G_g = G_0 \exp[-U^*/R(T_c - T_\infty)] \exp[-K_g/T_c(\Delta T)f] \quad (3)$$

where G_0 is a preexponential factor (independent of temperature), U^* is the activation energy for reptation in the melt (=1500 cal/mol), T_∞ is a theoretical temperature at which reptation ceases ($T_g = -30$ K), K_g is a nucleation constant, and $f = 2T_c/T_m^\circ + T_c$.

This equation can also be written as

$$\ln G_g = \ln G_0 - U^*/R(T_c - T_\infty) - K_g/T_c(\Delta T)f \quad (4)$$

If a plot of [$\ln G_g + U^*/R(T_c - T_\infty)$] as a function of $1/T_c(\Delta T)f$ results in a straight line, this will indicate that eq. (4) can describe with some precision the experimental G_g as a function of temperature.[20]

From the slopes of the straight lines, K_g and, consequently, σ_e can be calculated if σ, the lateral surface interfacial free energy, is known. These last parameters are related by the following equation:

$$K_g = rb\sigma\sigma_e T_m^\circ / \Delta H_m^\circ \kappa \quad (5)$$

where r is the parameter characteristic of the growth regime (its value will be 4 if the regimes are I or III and 2 if the regime is II), b is the thickness of the surface nucleus, ΔH_m° is the equilibrium heat of fusion, and κ is the Boltzmann constant.

The value of σ can be calculated from the Thomas–Staveley equation:

$$\sigma = \beta \Delta H_m^\circ A_0^{1/2} \quad (6)$$

where A_0 is the cross-sectional area of the chain and β is a constant equal to 0.1 for polyolefins and 0.24 for polyesters.[21,22]

From the unit cell dimensions, the σ of the PP was found to be 11.49 erg/cm^2.[14] Equation (6) was also used to calculate σ for other polymers and satisfactory results have been obtained.[23–25]

The main contribution to σ_e is given by the necessary work to fold the polymeric chain or work of folding (q), given by

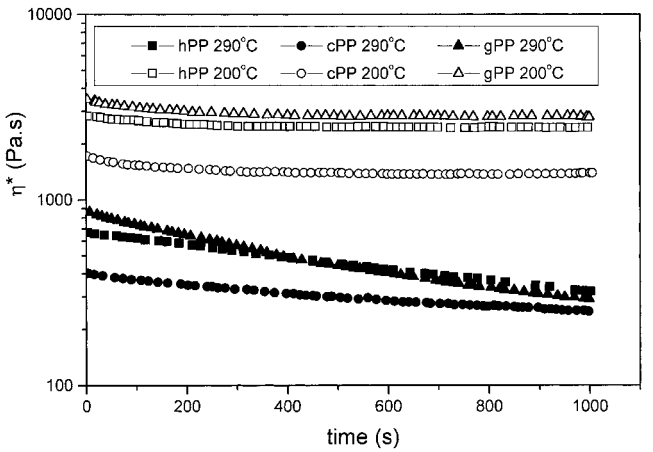

Figure 2 Complex viscosity as a function of time at the two melting conditions.

$$q = 2\sigma_e ab \tag{7}$$

where a is the width of the molecular chain.

The following values[21] were used for the calculation of the σ_e of the PP resins: $b = 6.26 \times 10^{-8}$ cm, $a = 5.49 \times 10^{-8}$ cm (110 growth plane), $\Delta H_m^\circ = 209$ J/g, $\sigma = 11.49$ erg/cm^2, and $r = 4$ (regime III).

Alternatively, the Avrami kinetic parameters n and k can also be related to G_g by the relation $G \sim k^{1/n}$, as mentioned earlier. G is the product of the nucleation and growth rates. Thus, to use eq. (4), the nucleation rate has to be considered to be much smaller than G_g and $G \cong G_g$. Therefore, eq. (4) can be written as

$$\alpha = \ln k/n + U^*/R(T_c - T_\infty) = \ln G_0 - rb\sigma\sigma_e T_m^\circ / \Delta H_m^\circ T_c \, \Delta T f \kappa \tag{8}$$

By plotting α as a function of $1/T_c(\Delta T)f$, σ_e can therefore be calculated. However, the values of σ_e, calculated by PLOM and DSC, will be different.

RESULTS AND DISCUSSION

Materials characterization

Figure 1(a) shows the FTIR spectra of the gPP and hPP resins, whereas Figure 1(b) shows the spectra of the cPP and hPP resins. From Figure 1(a) the gPP spectra shows a peak at 1710 cm^{-1}, corresponding to maleic anhydride (grafted and residual) in the cyclic form, thus confirming the MA grafting in the PP. From Figure 1(b) the cPP spectrum shows a small absorption band around 733 cm^{-1}, characteristic of random isolated ethylene units between propylene units.[26] The 720 and 729 cm^{-1} bands, characteristic of ethylene block copolymers, were not observed, thus confirming that the cPP is a random copolymer.

Figure 2 shows the $\eta^*(\omega)$ curves as a function of time. No preshear was applied to the samples; therefore the viscosity decrease up to near 100 s must be

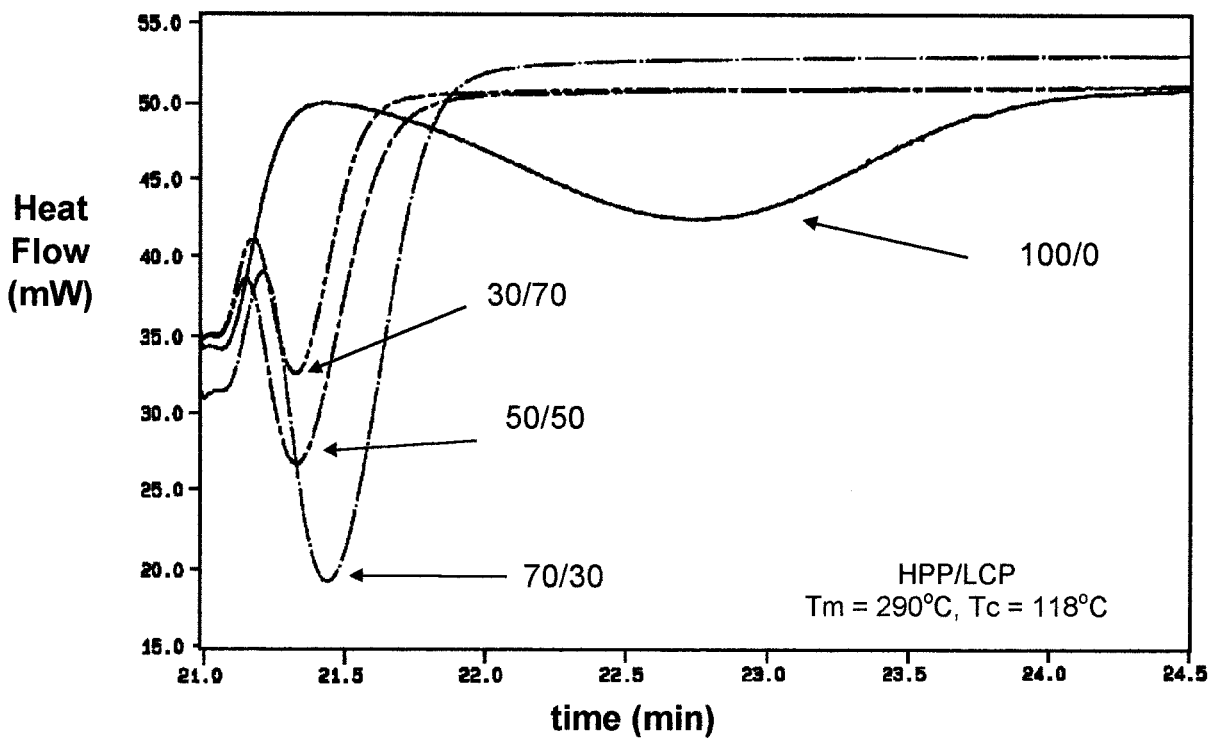

Figure 3 Standard DSC scannings of the isothermal crystallization of hPP/LCP blends at $T_c = 118$°C after melting at 290°C.

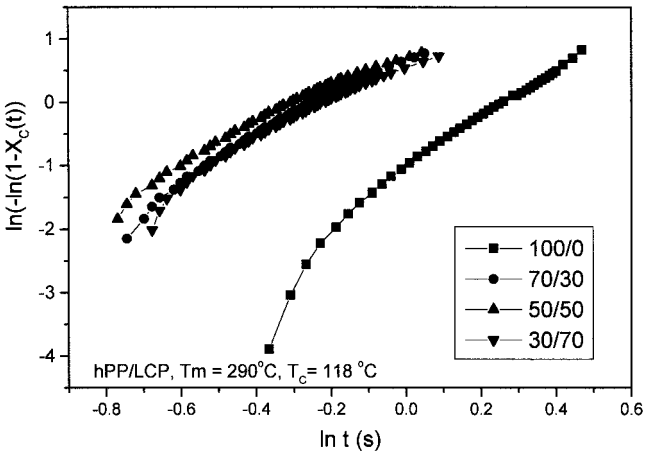

Figure 4 Standard Avrami curves for the hPP/LCP blends, at T_c = 118°C after melting at 290°C.

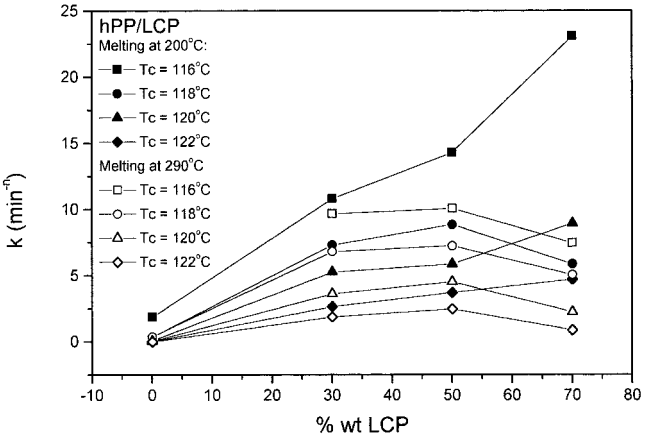

Figure 5 Overall crystallization rate k, obtained from the Avrami analysis of the hPP/LCP blends.

considered a result of the sample's disentanglement. After this time, at 200°C, there was no significant viscosity decrease in the samples; thus it is expected that at this temperature, no degradation of the PP resins will occur. At 290°C, however, all the PP resins showed a viscosity decrease. The gPP had the higher decrease; thus its degradation should be more intense than that of the other two. To avoid degradation of this resin, an antioxidant was used, as described in the Experimental section.

Isothermal crystallization

Avrami analysis

Figure 3 shows standard DSC curves of the hPP/LCP blends during isothermal crystallization, whereas Figure 4 shows the Avrami curves for the same blends, after melting at 290°C and at T_c = 118°C. The parameters n and k were calculated in the linear portion of the curve. Table II shows the n values, whereas Figures 5, 6, and 7 show the k parameters of all the blends.

At both values of T_m, n did not change significantly with T_c in all the blends; that is, T_c did not affect the dimensionality of the PP morphology in each blend. As is known,[16] if n = 4 or 3, the crystals are tridimensional, in the form of spheres; if n = 2 or 3, the crystals are two-dimensional, in the form of discs; if n = 2 or 1, the crystals are one-dimensional, in the form of rods.

For the hPP/LCP blends, as the LCP amount in the blends increased, n diminished, for both T_m values, going from the range of 2 to the range of 1. Thus a reduction in the dimensionality of the hPP crystals occurred as the amount of LCP in the blends increased.

Regarding k, the overall crystallization rate increased with the increase in the amount of supercooling, $\Delta T = T_m - T_c$, for both T_m values, as expected.

TABLE II
Blends Avrami Parameter *n*, as Calculated by DSC

		n			*n*			*n*	
T_c (°C)	Blend hPP/LCP	T_m = 200°C	T_m = 290°C	Blend cPP/LCP	T_m = 200°C	T_m = 290°C	Blend gPP/LCP	T_m = 200°C	T_m = 290°C
116	100/0	2.3	2.5	100/0	2.7	2.8	100/0	1.8	2.0
118		2.5	2.7		2.9	2.8		1.9	2.0
120		2.2	2.5		2.9	2.8		1.9	1.9
122		2.2	2.4		2.8	2.9		2.0	2.4
116	70/30	1.8	1.9	70/30	2.4	2.8	70/30	2.3	1.9
118		1.7	2.0		2.4	3.0		1.9	2.0
120		1.9	2.1		2.8	3.2		2.0	2.1
122		2.0	2.2		2.8	3.3		2.0	2.3
116	50/50	2.0	1.8	50/50	2.1	2.7	50/50	1.9	2.1
118		1.7	1.8		2.3	2.1		1.9	2.1
120		1.6	2.0		2.7	2.6		1.9	2.3
122		1.7	2.0		2.6	2.9		2.2	2.4
116	30/70	1.8	1.7	30/70	1.9	2.3	30/70	1.8	1.9
118		1.7	1.8		2.2	2.1		1.8	2.1
120		1.7	1.8		2.5	2.6		1.9	2.2
122		1.9	1.9		2.5	2.6		1.8	2.4

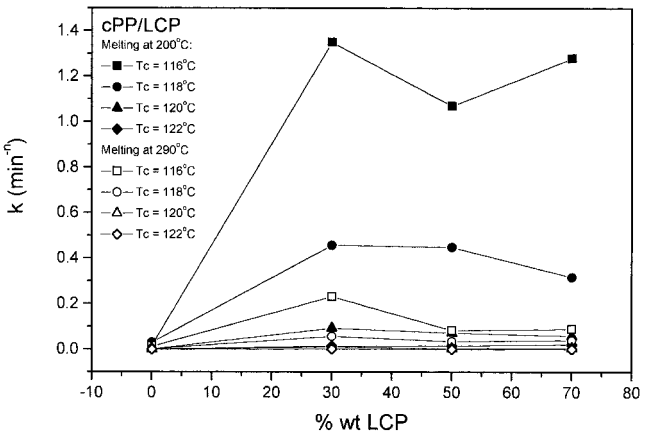

Figure 6 Overall crystallization rate k, obtained from the Avrami analysis of the cPP/LCP blends.

Also, the overall crystallization rates after T_m = 200°C are higher than those after T_m = 290°C. As already mentioned, at 290°C, the LCP melts and recrystallizes slowly: recrystallization originated from the unmelted small crystallites that are in the nematic melt. Thus the morphology of the LCP domains or crystallites after T_m = 290°C will be different from the morphology after T_m = 200°C. The crystallites that originated after T_m = 290°C probably will have smaller surface area (higher dimensions) because they were more slowly recrystallized than the crystallites already existing at T_m = 200°C, which were the result of the injection-molding process (fast cooling). Furthermore, the amount of LCP crystallites after T_m = 290°C will be lower than the amount of LCP crystallites at 200°C. These last LCP crystallites, because they are smaller and more numerous, will accelerate the overall crystallization rate.

At T_m = 200°C, as a rule, the overall crystallization rate of the hPP increased with the increase in the amount of LCP in the blend. The highest overall crystallization rates occurred at T_c = 116°C in the 70 wt % LCP composition; that is, the blend with the highest amount of LCP had the highest overall crystallization rate. This behavior can be credited to the nucleating effect of the LCP, given that this polymer was still in the solid state at 200°C (although k represents the sum of the nucleation and growth processes). This is the same effect that carbon and glass fibers have on PP.[27,28] This effect has also been observed in other blends with LCPs,[29,30] where transcrystallites around the LCP fibrils were observed.

At T_m = 290°C, the highest overall crystallization rate occurred at T_c = 116°C in the 50 wt % LCP composition; after this composition, the rate decreased. The increase of the rate up to 50 wt % LCP composition can be attributed to the nucleating effect of the LCP; the decrease of rate after this composition can be motivated by the high dispersion of the PP.

For the cPP/LCP blends, for T_m = 200°C, as the LCP amount in the blends increased, n diminished slightly, but still was in the range of 2. Therefore, the dimensionality of the cPP crystals was not strongly affected by the increase in the amount of LCP in the blends. At T_m = 290°C, n had different behavior: it was around 2, in the pure cPP, increased to 3 when 30 wt % LCP was added, and then decreased again up to 2.4. Therefore, the addition of 30 wt % LCP increased the dimensionality of the cPP crystals; however, after this concentration, this dimensionality was not affected.

Regarding k, the same behavior was observed with respect to the undercooling ΔT, as for the hPP blends. Also, the overall crystallization rates after T_m = 200°C were higher than those after T_m = 290°C, as occurred in the hPP blends.

At T_m = 200°C, as a rule, the overall crystallization rate of the cPP increased when the LCP was added to the blend up to an almost constant value; that is, this rate was independent of the amount of LCP in the blend.

At T_m = 290°C, the highest overall crystallization rate occurred at T_c = 116°C in the 30 wt % LCP composition. After this composition, this rate decreased to the values of the pure cPP.

Finally, in the gPP blends it was observed that n was not affected, either by the amount of LCP or the T_c, at both melting temperatures, having a constant value of 2.

Regarding k, the overall crystallization rates again are higher after melting at T_m = 200°C than those after T_m = 290°C, and, as a rule, this rate increased with the increase in the amount of LCP in the blend. The crystallization rates of the pure gPP at T_m = 200°C were almost twice the crystallization rate at T_m = 290°C.

The crystallization rates of the pure gPP and hPP polymers were much higher than that of the cPP, as expected, because cPP is a random copolymer.

From the Avrami analysis the overall crystallization rate obtained is the product of two processes, nucle-

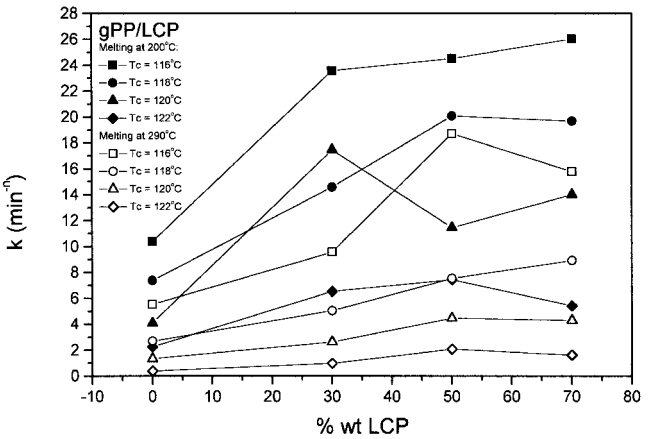

Figure 7 Overall crystallization rate k, obtained from the Avrami analysis of the gPP/LCP blends.

TABLE III
Induction Time for the Beginning of the Crystallization t_i, (in min)

Blend composition PP/LCP	T_c (°C)	hPP/LCP		cPP/LCP		gPP/LCP	
		T_m = 200°C	T_m = 290°C	T_m = 200°C	T_m = 290°C	T_m = 200°C	T_m = 290°C
100/0	116	0.33	0.35	0.47	0.54	0.21	0.26
	118	0.34	0.38	0.54	0.73	0.23	0.26
	120	0.40	0.41	0.53	0.72	0.28	0.26
	122	0.47	0.43	0.56	0.72	0.27	0.32
70/30	116	0.08	0.16	0.28	0.42	0.17	0.19
	118	0.11	0.17	0.35	0.48	0.17	0.23
	120	0.12	0.19	0.35	0.36	0.16	0.23
	122	0.12	0.20	0.35	0.34	0.21	0.29
50/50	116	0.05	0.13	0.33	0.57	0.18	0.19
	118	0.06	0.15	0.35	0.48	0.19	0.23
	120	0.08	0.13	0.36	0.48	0.20	0.20
	122	0.08	0.17	0.36	0.40	0.21	0.29
30/70	116	0.07	0.17	0.33	0.53	0.19	0.23
	118	0.08	0.19	0.39	0.60	0.20	0.24
	120	0.08	0.19	0.39	0.49	0.21	0.23
	122	0.12	0.24	0.38	0.43	0.23	0.25

ation and growth. Therefore, it is necessary to evaluate these two processes separately to analyze the influence of the LCP on the nucleation and growth rates of the PP.

To analyze the nucleation rate, the induction time for crystallization (t_i) was measured and is shown in Table III; as a rule, for all the blends, this induction time decreased, independent of the T_m, with the increase in the amount of LCP in the blend (i.e., the LCP reduced the time necessary for the PP resins to begin to crystallize), thus confirming the nucleating effect of the LCP. This behavior is the opposite of that found in blends of polyetheretherketone and another LCP, HX4000,[30] but is the same as that for blends of polyphenylene sulfide and this same HX4000.[29]

The nucleating effect, however, varied from resin to resin; at T_m = 200°C and, for T_c = 116°C, for example, in the 70/30 hPP/LCP blends, there was a reduction of the t_i of about 75%, whereas in the 70/30 cPP/LCP blend, this reduction was about 40% and in the 70/30 gPP/LCP blend it was about 20%. If the T_m and T_c are the same but one changes the blend composition, the same behavior is observed: in the 30/70 hPP/LCP blend the reduction of t_i is about 79%; in the 30/70 cPP/LCP blend it is about 30%; and in the 30/70 gPP/LCP blend it is about 10%. This same trend is observed in all the blends at both values of T_m and at all T_c values. Therefore, we conclude that the nucleating effect of the LCP was strong for the hPP and medium for the cPP and gPP resins.

The percentage of PP crystallinity, as a result of both isothermal crystallization experiments, was calculated using eq. (2), and the results are shown in Table IV.

Regarding the hPP/LCP blends, $X_{c,\mathrm{PP}} \cong 41\%$, for the pure hPP, independent of T_m; however, in the blends, after both melting conditions $X_{c,\mathrm{PP}}$ increased with the increase in the amount of LCP up to 50 wt % of LCP; after this concentration, the crystallinity slightly decreased.

Regarding the cPP/LCP blends, $X_{c,\mathrm{PP}} \cong 34\%$ for the pure cPP, independent of T_m; however, in the blends, after both melting conditions, $X_{c,\mathrm{PP}}$ slightly decreased up to 50 wt % of LCP, increasing after this concentration. Although the induction time for the beginning of the crystallization of this polymer was diminished with the addition of LCP, the total amount of crystallinity decreased slightly.

Regarding the gPP/LCP blends, $X_{c,\mathrm{PP}} \cong 46\%$ for the pure gPP, independent of T_m; however, in the blends, after both melting conditions, $X_{c,\mathrm{PP}}$ increased with the increase in the amount of LCP.

Finally, Figure 8 shows a standard Hoffman–Weeks plot for the gPP polymer and Table V shows the T_m° values for all the blends.

The T_m° values are extrapolated values; therefore, some accuracy is lost in its extrapolation. Within the range of experimental error, for the hPP blends, after T_m = 200°C, T_m° = 188°C, whereas after T_m = 290°C, T_m° = 196°C, showing that after these two melting conditions, these T_m° values were not strongly affected by blending with LCP and in the melt state these blends can be considered to be not miscible.

For the cPP blends, however, after both meltings, the T_m° values of the pure cPP resin were strongly decreased by the blending with the LCP, indicating that the cPP crystals formed in the blends were smaller and more imperfect than the crystals of the pure cPP, probably because of some plasticization or miscibility with the LCP molecules in the melt state.

For the gPP blends, a different trend was observed; after melting at T_m = 200°C, the resulting gPP crystals in the blends were smaller and more imperfect than

TABLE IV
Amount of PP Crystallinity $X_{c,\ PP}$ after Isothermal Crystallization, Determined by DSC (in %)

T_c (°C)	Blend hPP/LCP	$X_{c,\ PP}$ (after melting at 200°C)	$X_{c,\ PP}$ (after melting at 290°C)	Blend cPP/LCP	$X_{c,\ PP}$ (after melting at 200°C)	$X_{c,\ PP}$ (after melting at 290°C)	Blend gPP/LCP	$X_{c,\ PP}$ (after melting at 200°C)	$X_{c,\ PP}$ (after melting at 290°C)
116	100/0	41.2	42.1	100/0	33.6	33.7	100/0	48.6	47.5
118		41.9	40.0		33.2	34.1		47.2	45.9
120		40.6	41.9		34.0	34.0		47.3	45.3
122		40.7	44.5		33.6	33.7		44.1	45.9
116	70/30	52.0	46.8	70/30	29.5	30.0	70/30	61.9	51.1
118		50.7	47.3		30.4	32.3		56.6	51.0
120		46.8	46.6		32.1	32.6		50.4	49.2
122		47.7	46.6		33.3	33.2		50.3	51.6
116	50/50	59.4	45.2	50/50	27.0	29.6	50/50	59.3	51.3
118		59.4	48.5		25.6	28.2		54.6	52.2
120			45.6		27.0	28.9		51.6	51.0
122		59.4	41.7		28.3	27.9		47.4	50.4
116	30/70	45.8	44.7	30/70	32.8	34.4	30/70	59.2	46.3
118		43.5	38.5		31.0	37.1		50.4	49.8
120		43.5	38.3		30.0	31.5		49.3	47.1
122		39.5	45.0		30.4	32.0		43.6	45.9

the gPP pure crystals; however, after melting at T_m = 290°C, the blending with the LCP seemed not to alter the size and perfection of the gPP crystals.

From these DSC studies we make the following conclusions:

1. For the hPP polymer, there was an increase in the overall crystallization rate with the increase in the amount of LCP in the blend. The LCP exerted a strong nucleating effect on this resin. The amount of hPP crystallinity in the blends increased with the increase of the amount of LCP. It is expected, therefore, that the growth rate of hPP in the blends will also increase or, if it decreases, its absolute value will be lower than the nucleation rate.
2. For the cPP polymer, the overall crystallization rate in the blends was not affected by the increase in the amount of LCP. The LCP exerted a medium nucleating effect on this resin; also a decrease in the amount of cPP crystallinity in the blend was observed. Therefore the growth rate of the cPP in the blends should decrease, having an absolute value equal to the nucleation rate.
3. For the gPP polymer, again, an increase in the overall crystallization rate in the blends with the increase in the amount of LCP was seen. The LCP exerted a medium nucleating effect on this resin; an increase in the amount of LCP increased the amount of gPP crystallinity in the blends. Therefore the growth rate of the gPP in the blends should also increase or, if it decreases, its absolute value will be lower than its nucleation rate.

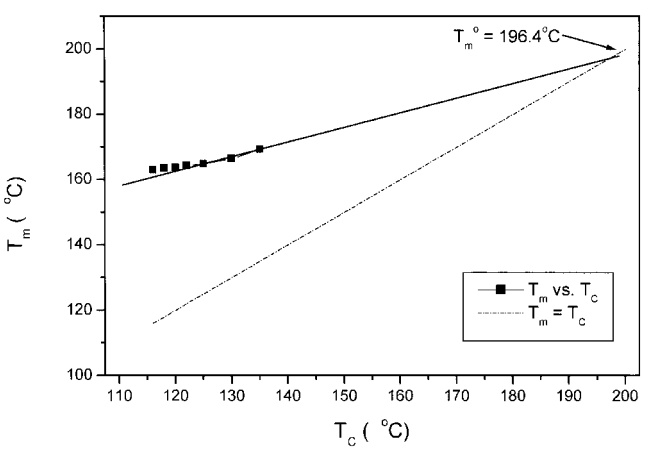

Figure 8 Standard Hoffman–Weeks plot for the gPP polymer.

TABLE V
T_m° of the Blends, as Determined by DSC

Blend	T_m° (°C), after T_m = 290°C	T_m° (°C), after T_m = 200°C
hPP/LCP		
100/0	196.7	188.6
70/30	192.2	191.0
50/50	192.4	191.7
30/70	195.3	188.2
cPP/LCP		
100/0	211.8	192.1
70/30	171.9	178.1
50/50	175.9	168.7
30/70	171.4	172.2
gPP/LCP		
100/0	196.4	201.3
70/30	201.2	191.0
50/50	194.0	188.0
30/70	195.3	180.0

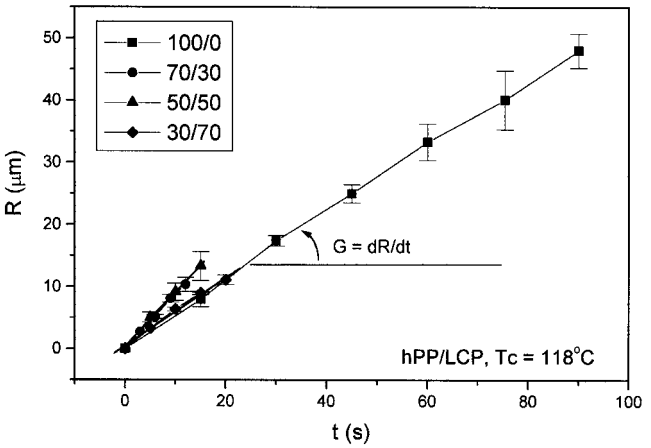

Figure 9 Standard spherulite radii curve of the hPP resin in the blends; the spherulite linear growth rate $G_g = dR/dt$.

Spherulites' isothermal linear growth rate, from PLOM

As described in the Experimental section, two melting conditions were used: 200 and 290°C. However, at 200°C, the PP crystallization occurred so fast that it was not possible to record the PLOM experiments to confirm the DSC results. Therefore, only the PLOM experiments at 290°C are presented here.

Figure 9 shows a typical spherulite radii curve of the hPP resin in the blends; the spherulite linear growth rate $G_g = dR/dt$. Figure 10 shows G_g (in μm/min) as a function of the crystallization temperature (T_c) for the blends.

As a rule, G_g decreased with the increase of T_c, as expected. The G_g of the hPP and gPP resins were much higher than that of the cPP. In the case of the hPP and gPP blends, the increase up to 50 wt % of LCP in the blends increased G_g, confirming the DSC results. For the cPP, however, G_g slightly decreased up to 50 wt % of LCP, also confirming the DSC results.

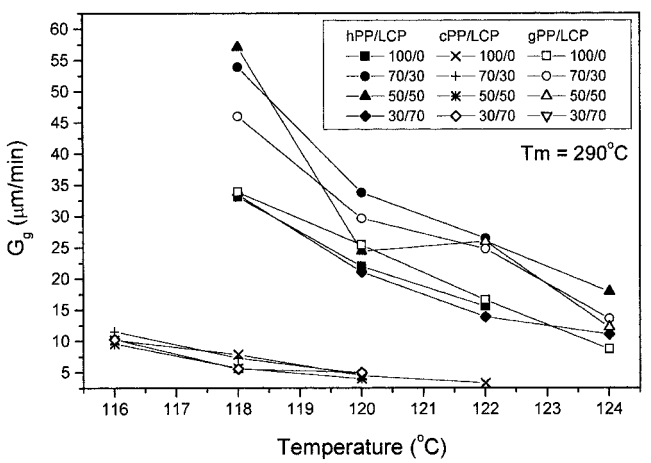

Figure 10 Linear growth rate G_g, as a function of the crystallization temperature T_c, for the blends.

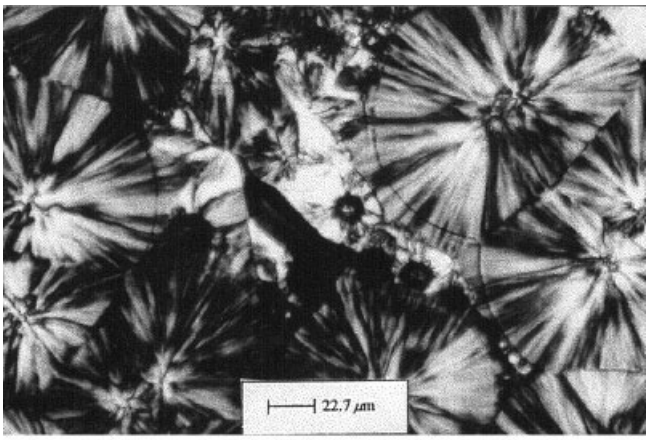

(a)

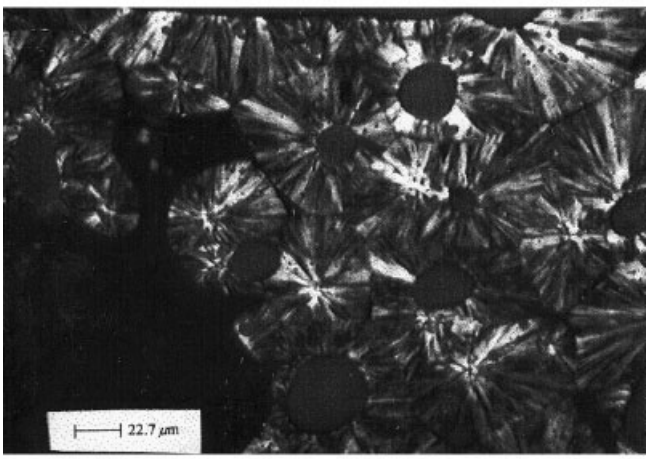

(b)

Figure 11 Final morphology: (a) hPP, T_c = 116°C; (b) hPP/LCP 70/30 blend, T_c = 122°C.

The final blend morphology, after these experiments, is also shown in Figures 11, 12, and 13. Figure 11(a) shows the pure hPP, whereas Figure 11(b) shows the 70/30 blend; Figure 12(a) shows the pure cPP, whereas Figure 12(b) shows the 50/50 blend; and, finally, Figure 13(a) shows the pure gPP, whereas Figure 13(b) shows the 70/30 blend. In all the figures, transcrystallinity of the PP resins around the LCP phase can be observed, confirming once more the nucleating effect that the LCP exerts over PP.

The pure gPP resin had three different populations of spherulites: (1) more perfect and large spherulites that grew from predetermined nuclei; (2) β-spherulites that grew from nuclei whose origins were small air bubbles trapped in the samples, identified because of their yellowish brightness; and (3) less perfect and smaller spherulites that grew from other nuclei that appeared instantaneously, as seen in Figure 13(b). To find out the reason for the surging of the third kind of spherulite population, the same crystallization experiments were run with virgin pellets of the pure gPP

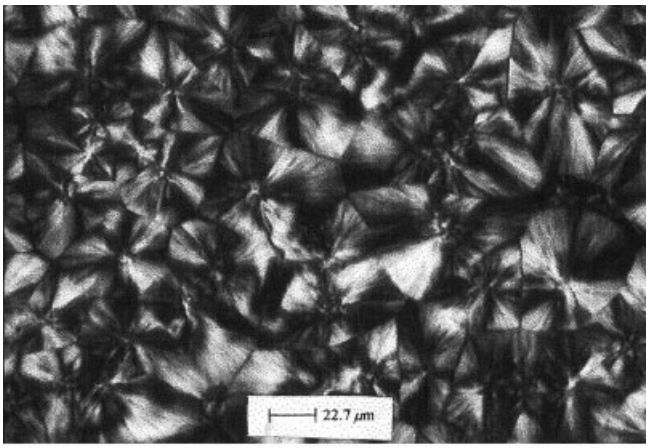

(a)

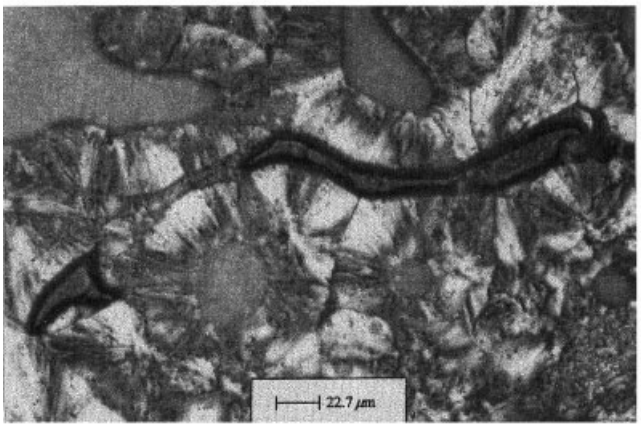

(b)

Figure 12 Final morphology: (a) cPP, T_c = 116°C; (b) cPP/LCP 50/50, T_c = 116°C.

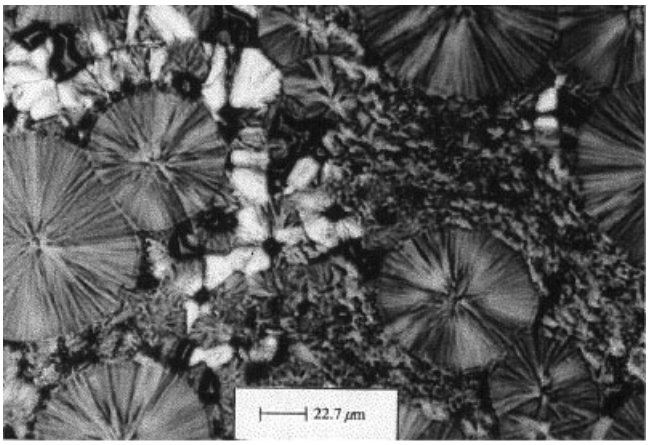

(a)

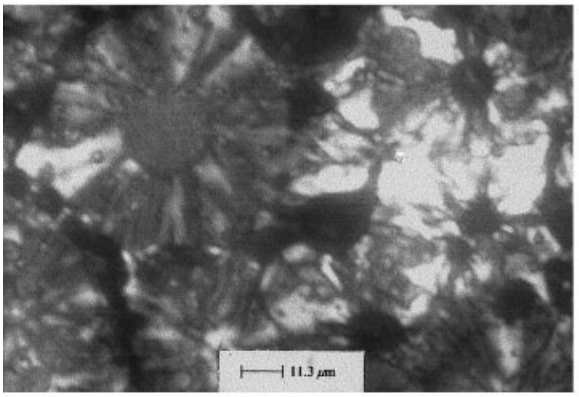

(b)

Figure 13 Final morphology: (a) gPP, T_c = 120°C; (b) gPP/LCP 70/30, T_c = 120°C.

resin that were not submitted to the injection-molding process. The resulting morphology is shown in Figure 14; this time, only the first and second kind of spherulites were observed. Therefore, the smaller spherulites of the injection-molded gPP resin, population 3, can be a consequence of the crystallization of low molecular weight gPP molecules. These low MW molecules can be a result of the gPP thermal degradation, and probably were expelled during the growth of the larger and more perfect spherulites.

When the LCP was added to the gPP resin, only the first and second population of gPP spherulites were seen, probably because the smaller spherulites were not allowed to grow. Either because of the LCP presence or because of the fast spherulite growth, the low molecular weight molecules did not have time to diffuse away to the growth front and were trapped intraspherulitically.

Glass-transition temperature

Figure 15 shows the DMTA of the blends and Table VI shows the transitions observed in the blends.

These values were obtained by deconvolution of the curves, using the Origin 5.0 software. In all the blends, two well-defined peaks of T_g values were observed: one corresponding to the PP resin and the other to the LCP. The T_g values of the hPP and gPP resins were

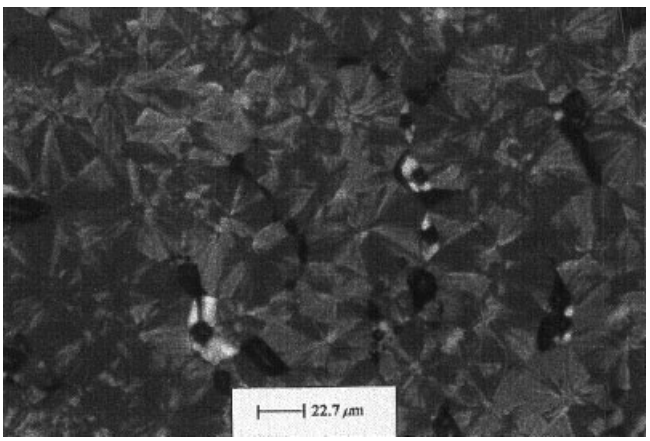

Figure 14 Final morphology of the gPP (virgin pellets), T_c = 120°C.

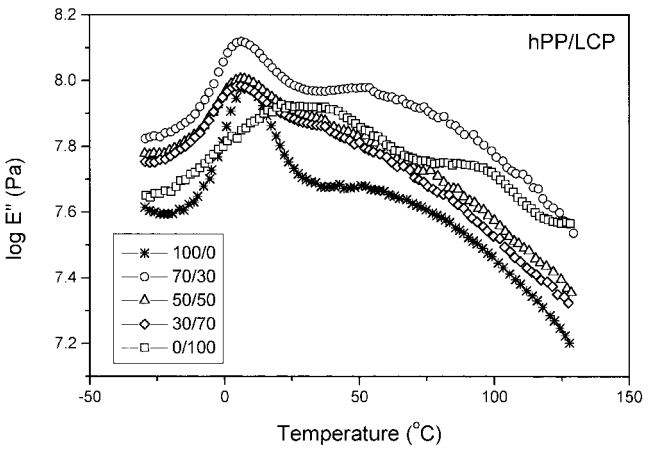

(a)

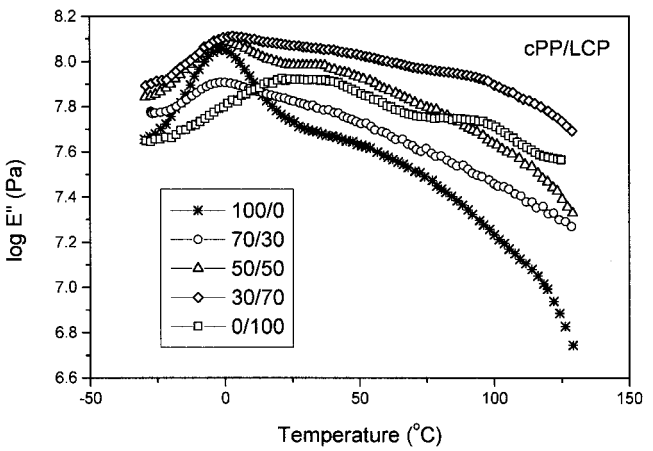

(b)

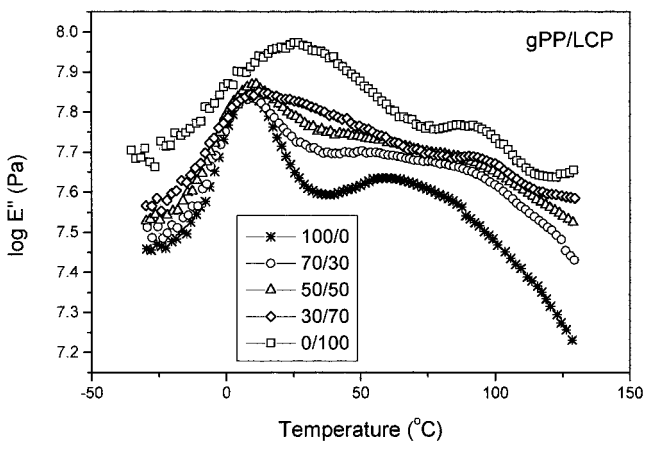

(c)

Figure 15 DMTA curves of the blends: (a) hPP/LCP; (b) cPP/LCP; (c) gPP/LCP).

located about 6.5°C and that of the cPP was about −2.3°C.

The T_g of the LCP in the hPP and gPP blends was about 88°C, having a small decrease from its original value (pure LCP). In the cPP blend the T_g has a value of 112°C, a small increase from its original value. A slight decrease of the LCP T_g was also observed in blends of PPS and another LCP,[29] attributed to a slight decrease in the amount of LCP crystallites arising from the inhibiting presence of the PP molecules. On the other hand, the increase of the LCP T_g in the cPP blends can be attributed to the formation of more LCP crystalline domains, facilitated by the dilution of the LCP molecules in a more flexible matrix (the cPP resin).

The decrease of $T_{\alpha,\mathrm{PP}}$ in the hPP and gPP blends can indicate that the intraspherulite amorphous parts became more flexible or more loosely attached during the crystallization process. This flexibility can be the result of the trapping of some LCP molecules during crystallization (small amounts of LCP have been used as plasticizers in thermoplastics[31,32]). However, the $T_{\beta,\mathrm{LCP}}$ did not change. In all cases, because two well-defined T_g values were found, the amorphous phases of both components in the solid state were immiscible.

Fold surface free energy

Figure 16 shows the $[\ln G + U^*/R(T_c - T_\infty)]$ versus $1/T_c(\Delta T)f$ plots for all the blends, as calculated from PLOM, after 290°C. From these graphs K_g and, subsequently, σ_e were calculated. Table VII, column (a), shows these values for all the blends.

Regarding the pure polymers, the cPP has the highest value of σ_e. For the blends, from column (a) of Table VII, the σ_e of the hPP and cPP blends decreased;

TABLE VI
Thermal Transitions of the Blends as Determined by DMTA

Sample	Thermal transitions (°C)[a]			
	T_g (PP)	$T_{\alpha'}$ (PP)	T_β (LCP)	T_g (LCP)
hPP/LCP				
100/0	7.9 (0.7)	64.7 (4.3)	—	—
70/30	6.0 (0.7)	48.2 (11.7)	29.0 (3.3)	94.2 (5.9)
50/50	7.6 (0.5)	48.7 (4.6)	32.4 (1.9)	84.6 (3.2)
30/70	4.5 (2.1)	58.8 (9.5)	30.9 (2.3)	90.4 (11.6)
cPP/LCP				
100/0	−1.5 (0.3)	66.6 (2.1)	—	—
70/30	−3.2 (0.3)	64.8 (6.1)	24.8 (5.3)	108.6 (6.6)
50/50	−1.8 (0.3)	70.4 (3)	30.9 (0.6)	115.0 (2.9)
30/70	−2.6 (0.7)	69.6 (6.4)	27.0 (2.8)	113.8 (10.3)
gPP/LCP				
100/0	7.5 (0.2)	76.6 (4.3)	—	—
70/30	6.8 (0.9)	50.4 (5.1)	29.1 (3.3)	82.5 (5.6)
50/50	6.8 (1.3)	49.8 (0.9)	26.4 (4.2)	87.2 (3.2)
30/70	5.0 (1.0)	54.1 (4.7)	24.4 (6.7)	94.8 (1.0)
LCP (Vectra A950)	—	—	28.2 (1.7)	93.1 (1.4)

[a] The values in parentheses represent the standard deviation.

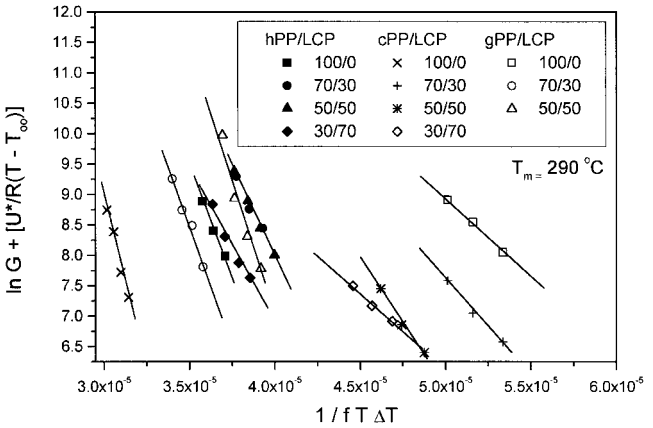

Figure 16 Hoffman–Lauritzen plots of the blends, obtained from PLOM data (T_m = 290°C).

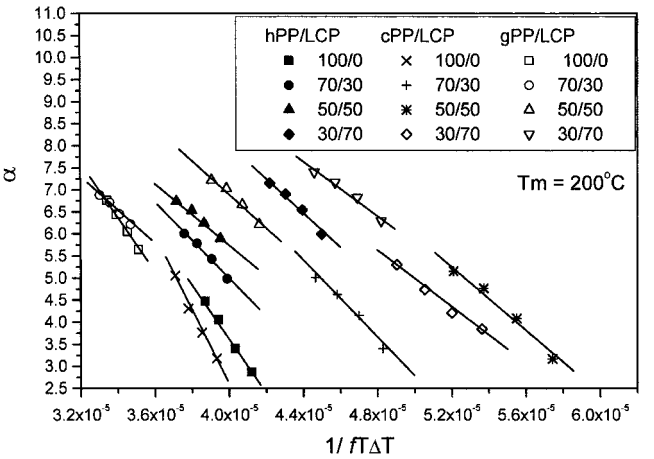

Figure 17 Hoffman–Lauritzen plots of the blends, obtained from DSC data (T_m = 200°C).

that is, less work was necessary to fold the PP molecule during crystallization when the LCP was present. However, the σ_e of the gPP in the blend increased; that is, more work was necessary to fold the gPP molecule in the crystal when the LCP was present.

Because, usually, PP crystallization studies are made from $T_m \ll 290$°C, our data could not be compared with other crystallization data. Thus, to allow the comparison of these data with data from the literature, we also calculated σ_e using the Avrami kinetic parameters n and k, as already described in the Experimental section. Figures 17 and 18 show the plots of α versus $1/T_c(\Delta T)f$ for all the blends, after melting at T_m = 200°C and T_m = 290°C, respectively. From the slopes of these lines, σ_e was calculated. Columns (b) and (c) of Table VII show these values.

The σ_e values of the pure hPP and cPP after melting at 200 and 290°C were different because σ_e depends on K_g, which itself depends on ΔT. The σ_e of the pure gPP, however, was not affected by the differences in ΔT. The final morphology of the pure PPs, after melting at 200 and 290°C, on the other hand, was the same. The values of n, the amount of final crystallinity, and the T_m° values of the pure PPs were the same, independent of the melting temperature; that is, even if the energy necessary to fold the polymeric chain changed with the melting temperature, the final morphology and crystallinity did not. This result confirms that the melt of the pure PPs was in the same thermodynamic condition (all the previous crystals were melted) at both melting temperatures.

The values at 290°C also were found to be different from the values calculated by PLOM because of the differences in measuring G.

The values of σ_e of the pure polymers at 200°C can be compared with data from the literature. It has been

TABLE VII
Values of σ_e, Calculated from PLOM and DSC Data

Blend	Calculated from PLOM data, T_m = 290°C (a) σ_e (erg/cm^2)	Calculated from DSC data, T_m = 200°C (b) σ_e (erg/cm^2)	Calculated from DSC data, T_m = 290°C (c) σ_e (erg/cm^2)
hPP/LCP			
100/0	137	138	254
70/30	113	91	105
50/50	105	97	97
30/70	114	86	144
cPP/LCP			
100/0	211	167	251
70/30	66	94	72
50/50	86	80	99
30/70	52	84	71
gPP/LCP			
100/0	133	132	100
70/30	153	87	164
50/50	198	81	124
30/70	—	64	148

estimated that for pure PP, σ_e = 65–70 erg/cm^2.[14] Table VIII shows some values of σ_e, after T_m = 200°C.[21]

The minimum value of σ_e of the pure hPP in Table VIII corresponds to the lower MW resin and the maximum value to the higher MW resin; in the case of the cPP, the maximum value of σ_e corresponds to the resin with higher percentage of ethylene (σ_e was found to be dependent on MW and % of ethylene). Our data at 200°C are similar to these values.[21]

Regarding the blends, the two techniques, PLOM and DSC, gave the same σ_e behavior: in the hPP and cPP blends σ_e decreased, whereas in the gPP blends, σ_e increased. The decrease of σ_e in the hPP and cPP blends can be attributed[33] to multiple nucleation that produced more nuclei and less folded chains, as observed from the DSC experiments for the hPP. The increase of σ_e in the gPP blends was unexpected: the difficulty to fold chains in the gPP blends can be a consequence of the probable chemical interaction between the grafted MA and the LCP, which would make folding more difficult. Note that the LCP modified the morphology of the gPP resin after melting at 290°C.

A comparison of the values of column (b) with the values of column (c), in general, for the hPP and gPP blends, shows that the values at 290°C were higher than the values at 200°C, whereas for the cPP, these values were similar. In other words, it was more difficult to fold the hPP and gPP chains after melting at 290°C, in the blends, than after melting at 200°C. For the cPP polymer, the melting temperature did not seem to affect the chain-folding energy. These results confirm the DSC measurements, which found that the overall crystallization rates of the blends after melting at 290°C were smaller than those after melting at 200°C.

At 290°C, both LCP and PP polymer resins melted. When cooling began, the LCP crystallized first, forming large crystallites. Probably because of the presence of these large LCP crystallites, the folding of the hPP and gPP resins during their crystallization was hindered. In the case of the cPP blends, because this polymer is a random copolymer, it would have low crystallinity. The dimensions and quantity of the LCP crystallites seem not to affect its crystallization, which will be dominated by its intrinsic chemical structure.

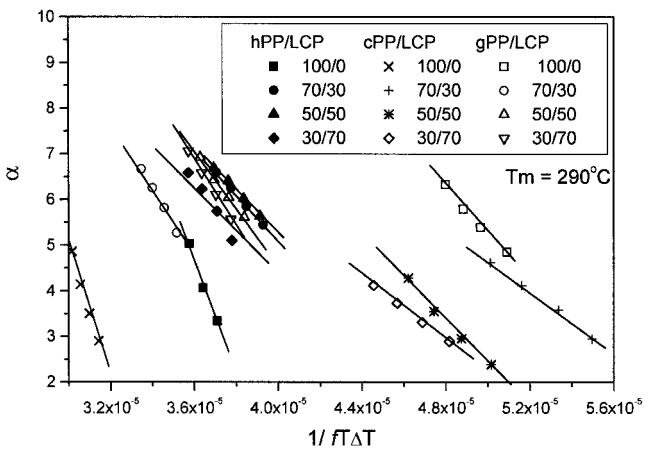

Figure 18 Hoffman–Lauritzen plots of the blends, obtained from DSC data (T_m = 290°C).

TABLE VIII
Values of σ_e, Calculated from DSC Data, After T_m = 200°C[a]

Pure hPP	Pure cPP	Pure gPP
75–134 erg/cm^2	111–141 erg/cm^2	134 erg/cm^2

[a] After de Carvalho and Bretas.[21]

CONCLUSIONS

The following preliminary conclusions can be inferred from this work:

1. The overall crystallization rates of the PP/LCP blends after T_m = 200°C were higher than those after T_m = 290°C, probably because the morphology of the LCP crystallites after each melting condition was different.
2. For the hPP polymer, there was an increase in the overall crystallization rate with the presence of the LCP. The LCP exerted a strong nucleating effect on this polymer and also increased its growth rate. As a result, an increase in the final percentage of crystallinity of the hPP in the blends was observed.
3. For the cPP polymer, the overall crystallization rate in the blends was not affected by the presence of the LCP. The LCP, however, exerted a medium nucleating effect on this resin. There was a slight decrease in the growth rate of cPP with the increase in the LCP amount of the blend. As a result, a decrease in the amount of cPP crystallinity in the blend was observed.
4. For the gPP polymer, an increase in the overall crystallization rate in the blends attributed to the presence of the LCP was seen. The LCP also exerted a medium nucleating effect on this resin. The growth rate was observed to increase with the amount of LCP in the blend. As a result, an increase in the final gPP crystallinity in the blends was observed.
5. After T_m = 290°C, the fold surface free energy of hPP and cPP in the blends decreased. On the other hand, this free energy increased in the gPP blends. The values of this energy after T_m = 290°C for the hPP and gPP blends were higher than the values after T_m = 200°C, whereas for the

cPP blends, these values were similar, confirming the DSC results (Conclusion 1).

6. All the PP resins formed transcrystallites on the surface of LCP domains.

The authors thank PRONEX and FAPESP for their financial aid and OPP Petrochemical of Brazil, for the donation of the samples.

References

1. Charrier, J. M. Polymeric Materials and Processing. Plastics, Elastomers and Composites; Hanser: New York, 1990.
2. O'Donnell, H. J.; Baird, D. G. Polymer 1995, 36, 3113.
3. Handlos, A. A.; Baird, D. G. Int Polym Process 1996, XI, 82.
4. Postema, A. R.; Fennis, P. J. Polymer 1997, 38, 5557.
5. Kozlowski, M.; La Mantia, F. P. J Appl Polym Sci 1997, 66, 969.
6. Marosi, G.; Bertalan, G.; Anna, P.; Tohl, A.; Lágner, R.; Balogh, I.; La Mantia, P. F. J Therm Anal 1996, 47, 1155.
7. Tjong, S. C.; Chen, S. X.; Li, R. K. Y. J Appl Polym Sci 1997, 64, 707.
8. Miteva, T.; Minkova, L. Macromol Chem Phys 1998, 199, 597.
9. Miteva, T.; Minkova, L.; Magagnini, P. Macromol Chem Phys 1998, 199, 1519.
10. da Silva, L.; Bretas, R. E. S. Polym Eng Sci 2000, 40, 1414.
11. Weinkauf, D. H.; Paul, D. R. J Polym Sci Part B: Polym Phys 1991, 29, 329.
12. Wunderlich, B. Macromolecular Physics, Vol. 2; Academic Press: New York, 1976; p 147.
13. Langelaan, H. C.; Postherma de Boer, A. Polymer 1996, 35, 5667.
14. Clark, E. J.; Hoffman, J. D. Macromolecules 1984, 17, 87.
15. Hoffmann, J. D.; Weeks, J. J. J Res A Phys Chem 1962, 66A, 13.
16. Sperling, L. H. Introduction to Physical Polymer Science, 2nd ed.; Wiley: New York, 1992.
17. Petraccone, V.; Guerra, G.; de Rosa, C.; Tuzi, A. Macromolecules 1985, 18, 813.
18. Tiganis, B. E.; Shanks, R. A.; Long, Y. J Appl Polym Sci 1996, 59, 663.
19. Weinkauf, D. H.; Paul, D. R. J Polym Sci Part B: Polym Phys 1992, 30, 837.
20. Hoffman, J. D.; Davi, G. T.; Lauritzen, J. I., Jr. In: Treatise on Solid State Chemistry; Hannay, N. B., Ed.; Plenum Press: New York, 1976; Vol. 3, Chapter 7.
21. de Carvalho, B.; Bretas, R. E. S. J Appl Polym Sci 1998, 68, 1159.
22. Martuscelli, E. Polym Eng Sci 1984, 24, 8.
23. Gabellini, G.; de Moraes, M. B.; Bretas, R. E. S. J Appl Polym Sci 1996, 60, 21.
24. Hsiao, B. S.; Sauer, B. B. J Polym Sci Part B: Polym Phys 1993, 31, 901.
25. Alfonso, G. C.; Chiappa, V.; Liu, J.; Sadiku, E. R. Eur Polym J 1991, 27, 795.
26. de Carvalho, B.; Bretas, R. E. S. J Appl Polym Sci 1999, 72, 1741.
27. Wang, C.; Liu, C. R. Polymer 1997, 38, 4715.
28. Arroyo, M.; López-Manchado, A.; Avalos, F. Polymer 1997, 38, 5587.
29. Gabellini, G.; Bretas, R. E. S. J Appl Polym Sci 1996, 61, 1803.
30. de Carvalho, B.; Bretas, R. E. S. J Appl Polym Sci 1995, 55, 233.
31. Choi, D. G.; Jo, W. H.; Kim, H. G. J Appl Polym Sci 1996, 59, 443.
32. Turek, D. E.; Simon, G. P.; Tiu, C.; Tiek-Siang, O. Polymer 1992, 33, 4322.
33. Lim, G. B. A.; Lloyd, D. R. Polym Eng Sci 1993, 33, 9513.